Volume 9, Number 8
1009-1963/2000/09(08)/0599-07
CHINESE PHYSICS
August, 2000
© 2000 Chin. Phys. Soc.

PHASE FLUCTUATIONS ON RAMAN-ENHANCED NONDEGENERATE FOUR-WAVE MIXING*

Zhang Yan-peng(张彦鹏), Wu Hong-cai(吴洪才),
Wnag Peng-fei(王鹏飞), and Li Chuang-she(李创社)
Department of Electronic Science and Technology, Xi'an Jiaotong University, Xi'an 710049, *China*
Fu Pan-ming(傅盘铭)
Institute of Physics, Chinese Academy of Sciences, Beijing 100080, *China*

(Received 21 December 1999; revised manuscript received 21 February 2000)

We have employed phase-diffusion model to study the effects of laser field correlation on the Raman-enhanced nondegenerate four-wave mixing (RENFWM). The different roles of the field fluctuations have been pointed out. A time-delayed method has been proposed to suppress the thermal background. An enhancement of the ratio between the resonant and nonresonant RENFWM signal intensities was found as the time delay is increased when the laser has broadband linewidth. When the lasers have Gaussian line shape, we also present a second-order coherence function theory to elucidate the temporal asymmetry behavior of the RENFWM.

Keywords: phase fluctuations, raman-enhancedment, four-wave mixing
PACC: 4265, 3290

I. INTRODUCTION

Recently, a large amount of work has been devoted to the effects of optical field fluctuations in nonlinear optics. It is well known that the influence of laser linewidths is more than just providing an additional broadening mechanism when the signal depends on higher than second order electric-field correlation.[1] Much attention has been paid to the four-wave mixing (FWM) with correlated fields. Optical transients induced by time-delayed correlated fluctuating pulses have been proved to be a powerful technique in obtaining subpicosecond time resolution.[2,3] This time resolution is determined by the coherence time of the fluctuating field. The field correlation can also affect one-photon and two-photon transitions. In the case of a nearly Lorentzian laser power spectrum, the width of the two-photon absorption spectrum is decreased when the counter-propagating laser beams are partially decorrelated. On the other hand, in an experiment of probe absorption due to atoms saturated by the strong pump, gain was observed when there was a time delay between the phase-diffusing pump and probe.[4]

Raman-enhanced nondegenerate four-wave mixing (RENFWM) is a third-order nonlinear phenomenon with phase-conjugation geometry.[5] It possesses the advantages of nonresonant background suppression, excellent spatial resolution, free choice of interaction volume, and simple optical alignment. Furthermore, there are three incident beams involved in RENFWM in which two of them originate from a single laser source. Therefore, by its very nature, RENFWM offers the possibility of studying the effect of field correlation. Fu *et al.*[6] also performed time-delayed RENFWM with incoherent light to measure the vibrational dephasing time. In this paper, we assume that the laser sources are phase-diffusing models, which are used to describe an amplitude-stabilized laser source with Lorentzian line shape. This model assumes that the amplitude of the laser field is a constant, while its phase fluctuates as random process. We have employed phase-diffusion model to study the effects of laser field correlation in RENFWM. The different roles of the field fluctuations have been pointed out. A time-delayed method has been proposed to suppress the thermal background. An enhancement of the ratio between the resonant and nonresonant RENFWM signal intensities was found as the time delay is increased when the laser has broadband linewidth. When the lasers have Gaussian line shape, we also present a second-order coherence function theory to elucidate the temporal asymmetry behavior of the RENFWM.

* Project supported by the National Natural Science Foundation of China (Grant No. 69978019).

Ⅱ. BASIC THEORY

RENFWM is a third-order nonlinear phenomenon with three incident beams involved. Beams 1 and 2 have the same frequency $\omega_1$and a small angle exit between them. Beam 3 with frequency ω_3 is almost propagating along the opposite direction of beam 1. In an absorbing liquid, the nonlinear interaction of beams 1 and 2 with the medium gives rise to a molecular-reorientational grating and a thermal grating. The FWM signal is the result of the diffraction of beam 3 by two small-angle static gratings. Now, if $|\omega_1 - \omega_3|$ is near the Raman resonant frequency Ω_R, a large-angle moving grating formed by the interference of beams 2 and 3 will excite the Raman-active vibrational mode of the medium and enhance the FWM signal. The FWM signal (beam 4) has frequency ω_3 and is propagating along the opposite direction of beam 2 approximately. The complex incident laser fields can be written as

$$\begin{aligned} E_i(\boldsymbol{r},t) &= A_i(\boldsymbol{r},t)\exp(-i\omega_i t) \\ &= \varepsilon_i u_i(t)\exp[i(\boldsymbol{k}_i\cdot\boldsymbol{r}-\omega_i t)](i=1,2,3), \end{aligned} \tag{1}$$

where $A_i(\boldsymbol{r},t) = \varepsilon_i u_i(t)\exp i(\boldsymbol{k}_i\cdot\boldsymbol{r})$; ω_i and $\boldsymbol{k}_i$ are the constant field amplitude and the wave vector of the ith beam, respectively, and $u_i(t)$ is a dimensionless statistical factor that contains phase and amplitude fluctuations.

According to Ref.[5] the total polarization responsible for the RENFWM signal, is given by

$$P^{(3)}(\boldsymbol{r},t) = P_M(\boldsymbol{r},t) + P_T(\boldsymbol{r},t) + P_R(\boldsymbol{r},t) \tag{2}$$

with

$$\begin{aligned} P_M(\boldsymbol{r},t) &= S(\boldsymbol{r},t)\chi_M\gamma_M A_3(t)\int_0^\infty \mathrm{d}t' A_1(t-t')A_2^*(t-t')\exp(-\gamma_M t') \\ &= \varepsilon_1(\varepsilon_2)^*\varepsilon_3 S(\boldsymbol{r},t)\chi_M\gamma_M u_3(t)\int_0^\infty \mathrm{d}t' u_1(t-t')u_2^*(t-t')\exp(-\gamma_M t'), \end{aligned} \tag{3}$$

$$\begin{aligned} P_T(\boldsymbol{r},t) &= S(\boldsymbol{r},t)\chi_T\gamma_T A_3(t)\int_0^\infty \mathrm{d}t' A_1(t-t')A_2^*(t-t')\exp(-\gamma_T t') \\ &= \varepsilon_1(\varepsilon_2)^*\varepsilon_3 S(\boldsymbol{r},t)\chi_T\gamma_T u_3(t)\int_0^\infty \mathrm{d}t' u_1(t-t')u_2^*(t-t')\exp(-\gamma_T t'), \end{aligned} \tag{4}$$

$$\begin{aligned} P_R(\boldsymbol{r},t) &= iS(\boldsymbol{r},t)\chi_R\gamma_R A_1(t)\int_0^\infty \mathrm{d}t' A_2^*(t-t')A_3(t-t')\exp[-(\gamma_R - i\Delta)t'] \\ &= i\varepsilon_1(\varepsilon_2)^*\varepsilon_3 S(\boldsymbol{r},t)\chi_R\gamma_R u_1(t)\int_0^\infty \mathrm{d}t' u_2^*(t-t')u_3(t-t')\exp[-(\gamma_R - i\Delta)t']. \end{aligned} \tag{5}$$

Here, $P_M(\boldsymbol{r},t)$, $P_T(\boldsymbol{r},t)$ and $P_R(\boldsymbol{r},t)$ are the nonlinear polarizations originating from the molecular-reorientational grating, the thermal grating, and the Raman-active mode, respectively; $\Delta = |\omega_1 - \omega_3| - \Omega_R$; $S(\boldsymbol{r},t) = \exp\{i[\boldsymbol{k}_1 - \boldsymbol{k}_2 + \boldsymbol{k}_3)\cdot\boldsymbol{r} - \omega_3 t]\}$; γ_M and χ_M (γ_T and χ_T, γ_R and χ_R) are the relaxation rate and the nonlinear susceptibility of the molecular-reorientational grating (the thermal grating, the Raman-active mode), respectively. Physically, integration effects are involved in the establishment of the molecular-reorientational grating, the thermal grating, and the Raman-active mode. The integrals in Eqs. (3)–(5) reflect these facts. On the other hand, the probing of the molecular-reorientational grating, the thermal grating, and the Raman-active mode are instantaneous processes. In our case, beams 1 and 2 come from a single laser source. Letting τ be the time delay of beam 2 with respect to beam 1, we have $u_1(t) = u(t), u_2(t) = u(t-\tau)$. The FWM signal is proportional to the average of the absolute square of $P^{(3)}$ over the random variable of the stochastic process, i.e., $I(\Delta,\tau) \propto < |P^{(3)}|^2 >$, which involves fourth- and second-order coherence functions of $u(t)$ in phase-conjugation geometry, while the FWM signal intensity in self-diffraction geometry is related to the sixth-order coherence function of the incident fields.[7] Commonly used stochastic model is phase-diffusion model, which is used to describe an amplitude-stabilized laser source. This model assumes that the amplitude of the laser field is a constant, while its phase fluctuates as random process. Fu *et al.*[5] assumed that the laser sources are chaotic fields. A chaotic field, used to describe a multimode laser source, is characterized by the fluctuation of both the amplitude and the phase of

the field. For the phase-diffusion model,[8] the fourth-order coherence function is

$$\begin{aligned} &< u(t_1)u(t_2)u^*(t_3)u^*(t_4) > \\ =&\exp[-\alpha(|t_1-t_3|+|t_1-t_4|+|t_2-t_3|+|t_2-t_4|)] \\ &\exp[\alpha(|t_1-t_2|+|t_3-t_4|)]. \end{aligned} \tag{6}$$

If beam 3 has Lorentzian line shape, we have the second-order coherence function

$$< u_3(t_1)u_3^*(t_2) >= \exp(-\alpha|t_1-t_2|), \tag{7}$$

where $\alpha = \frac{1}{2}\delta\omega_1, \alpha_3 = \frac{1}{2}\delta\omega_3$ with $\delta\omega_1$ and $\delta\omega_3$ being the laser linewidths of beams 1 and 3.

Substituting Eqs. (6) and (7) into $I(\Delta,\tau) \propto< |P^{(3)}|^2 >$ and performing the tedious integration, we obtain, for $\tau > 0$,

$$\begin{aligned} I(\Delta,\tau) \propto& \frac{\chi_M^2\gamma_M}{\gamma_M+2\alpha} + \frac{\chi_T^2\gamma_T}{\gamma_T+2\alpha} + \frac{\chi_R^2\gamma_R(\gamma_R+\alpha+\alpha_3)}{(\gamma_R+\alpha+\alpha_3)^2+\Delta^2} \\ &+ \frac{\chi_M\chi_T\gamma_M\gamma_T(3\gamma_M+3\gamma_T+4\alpha)}{(\gamma_M+\gamma_T)(\gamma_M+2\alpha)(\gamma_T+2\alpha)} - \frac{2\chi_M\chi_R\gamma_M\gamma_R\Delta}{(\gamma_M+\gamma_R+\alpha+\alpha_3)^2+\Delta^2} \\ &\times\left[\frac{\gamma_M+2(\gamma_R+\alpha+\alpha_3)}{(\gamma_R+\alpha+\alpha_3)^2+\Delta^2}+\frac{1}{\gamma_M+2\alpha}\right] - \frac{2\chi_T\chi_R\gamma_T\gamma_R\Delta}{(\gamma_T+\gamma_R+\alpha+\alpha_3)^2+\Delta^2}\left[\frac{\gamma_T+2(\gamma_R+\alpha+\alpha_3)}{(\gamma_R+\alpha+\alpha_3)^2+\Delta^2}+\frac{1}{\gamma_T+2\alpha}\right] \\ &+\left\{\frac{2\chi_M^2\alpha}{\gamma_M+2\alpha}+\frac{4\chi_M\chi_T\gamma_T\alpha}{(\gamma_M+\gamma_T)(\gamma_M+2\alpha)}-\frac{4\chi_M\chi_R\gamma_R\alpha\Delta}{(\gamma_M+2\alpha)[(\gamma_M+\gamma_R+\alpha+\alpha_3)^2+\Delta^2]}\right\}\exp[-(\gamma_M+2\alpha)|\tau|] \\ &+\left\{\frac{2\chi_T^2\alpha}{\gamma_T+2\alpha}+\frac{4\chi_M\chi_T\gamma_M\alpha}{(\gamma_M+\gamma_T)(\gamma_T+2\alpha)}-\frac{4\chi_T\chi_R\gamma_R\alpha\Delta}{(\gamma_T+2\alpha)[(\gamma_T+\gamma_R+\alpha+\alpha_3)^2+\Delta^2]}\right\}\exp[-(\gamma_T+2\alpha)|\tau|]. \end{aligned} \tag{8}$$

In general, the RENFWM spectra are different for $\tau > 0$ and $\tau < 0$. Physically, when $|\tau| \to \infty$, beams 1 and 2 are mutually incoherent, therefore, whether τ is positive or negative does not affect the RENFWM spectrum.

Ⅲ. SUPPRESSION OF THERMAL BACKGROUND BY A TIME-DELAYED METHOD

The basic principle of the time-delayed method to suppress the thermal background is the following. Consider a nondegenerate FWM experiment with beams 1 and 2 coming from a single laser source and having the same polarization. The interference pattern of beams 1 and 2 will be in constant motion when the relative time delay between them is much longer than the laser coherence time. Now, we choose the laser linewidth such that $\gamma_M > \alpha \gg \gamma_T$. Because the phase of the interference pattern changes randomly on the scale of the laser coherence time, the integrated effect will wash out the thermal grating completely. On the other hand, the molecular-reorientational grating has much shorter relaxation time. It will follow the randomly moved field interference pattern and therefore still exist. In the RENFWM, the FWM signal has three origins, i.e., molecular reorientation, thermal effect, and Raman vibration. We are interested in RENFWM spectrum. When $\Delta = 0$, the excitation of the Raman active mode leads to a resonant structure in the spectrum. In contrast, the molecular-reorientational grating and the thermal grating give rise to a nonresonant background. When we increase the relative time delay between beams 1 and 2, the nonresonant background decreases due to the elimination of the thermal background. We consider the case that $\gamma_M, \gamma_R > \alpha \gg \gamma_T$ and $(\chi_T/\chi_M)^2(\gamma_T/2\alpha) \ll 1$, the thermal background can be eliminated completely when the relative time delay is much longer than the laser coherence time. Our numerical results are given in Fig. 1. For a typical sample, the relaxation time of the thermal grating is on the order of microsecond, while the Debye relaxation time is only a few picoseconds; therefore, it is reasonable to use the following parameters in the calculation: $\chi_M/\chi_R = 0.2$; $\chi_T/\chi_R = 10$; $\gamma_M/\alpha = \gamma_R/\alpha = 10$; $\gamma_T/\alpha = 1 \times 10^{-5}$; $(\chi_T/\chi_M)^2(\gamma_T/2\alpha) = 0.0125$, and $\alpha_3/\alpha = 1$. When $\alpha\tau = 0$, a huge nonresonant background originating from the thermal grating exists in the RENFWM spectrum, which obscures the Raman resonance signal. However, the nonresonant background decreases drastically as $\alpha\tau$ increases. At $\alpha\tau = 10$, the RENFWM spectrum converts to the corresponding RENFWM spectrum of a nonabsorbing sample, which has the same parameters except χ_T=0. On the other hand, the theoretical RENFWM spectra show the normal asymmetry due to the interference between the Raman resonant term and the nonresonant background

originating solely from the molecular-reorientational grating. Although thermal gratings can be eliminated by using a cross-polarization configuration for beams 1 and 2, we note that, since the population grating can be generated only when beams 1 and 2 have the same polarization, the cross-polarization configuration is not helpful in distinguishing population gratings from thermal gratings.

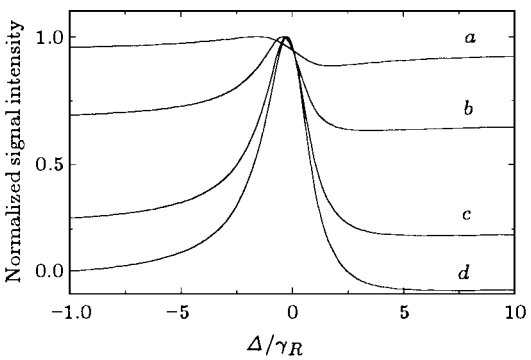


Fig.1. Normalized RENFWM signal intensity versus Δ/γ_R for the different relative time delay. Parameters: $\chi_M/\chi_R = 0.2$; $\chi_T/\chi_R = 10$; $\gamma_M/\alpha = \gamma_R/\alpha = 10$; $\gamma_T/\alpha = 1\times10^{-5}$; $\alpha_3/\alpha = 1$ and (a) $\alpha\tau = 0$; (b) $\alpha\tau = 2$; (c) $\alpha\tau = 3$; (d) $\alpha\tau = 10$.

IV. EFFECTS OF FIELD-CORRELATION ON RENFWM

In a nonabsorbing sample ($\chi_T = 0$), Eq. (8) becomes

$$
\begin{aligned}
I(\Delta,\tau) \propto \chi_M^2 \Bigg\{ & \frac{\gamma_M}{\gamma_M+2\alpha} \\
& + \frac{2\alpha}{\gamma_M+2\alpha}\exp[-(\gamma_M+2\alpha)|\tau|]\Bigg\} \\
& + \chi_R^2 \frac{\gamma_R(\gamma_R+\alpha+\alpha_3)}{(\gamma_R+\alpha+\alpha_3)^2+\Delta^2} - 2\chi_M\chi_R \\
& \times \Bigg\{ \frac{\gamma_M\gamma_R\Delta}{(\gamma_M+\gamma_R+\alpha+\alpha_3)^2+\Delta^2}\Bigg[\frac{\gamma_M+2(\gamma_R+\alpha+\alpha_3)}{(\gamma_R+\alpha+\alpha_3)^2+\Delta^2} \\
& + \frac{1}{\gamma_M+2\alpha}\Bigg] + \frac{2\gamma_R\alpha\Delta}{(\gamma_M+2\alpha)[(\gamma_M+\gamma_R+\alpha+\alpha_3)^2+\Delta^2]} \\
& \times \exp[-(\gamma_M+2\alpha)|\tau|]\Bigg\} = \chi_M^2 F_M(\tau) \\
& + \chi_R^2 F_R(\Delta) - 2\chi_M\chi_R F_{RM}(\Delta,\tau). \qquad (9)
\end{aligned}
$$

Here, $F_M(\tau)$, $F_R(\Delta)$, and $F_{RM}(\Delta,\tau)$ are functions which correspond to the FWM signal originating from the molecular-reorientational grating, the Raman-active mode, and the interference between the molecular-reorientational grating and the Raman resonance, respectively. They depend on the statistics of the laser fields. We assume that the lasers are the amplitude-stabilized laser sources with Lorentizan line shape.

We first study the temporal behavior of the molecular-reorientational grating. Figure 2 presents theoretical curve of $F_M(\tau)/F_M(0)$ versus $\alpha\tau$, where the values of γ_M/α, which equal 100, 1, and 0.01, are given in the figure. The phase of the interference pattern of beams 1 and 2, i.e., the phase factor $\Phi_M(\tau)$ of $A_1(t-t')A_2^*(t-t')$ in Eq. (3), changes from 0 to a random variable which fluctuates with characteristic time scale of the laser coherence time $\tau_c \approx \alpha^{-1}$ when τ is varied from 0 to ∞. The effect of integration in the establishment of the molecular-reorientational grating, which last for a duration of approximately the relaxation time of the molecular-reorientational grating $\tau_M \approx \gamma_M^{-1}$, is to wash out the grating when $\tau \neq 0$. When $\tau_M \gg \tau_c$ the molecular-reorientational grating will be washed out completely as $\tau \to \infty$ and we have $F_M(\tau) \propto \exp(-2\alpha|\tau|)$ in this limit (curve with γ_M/α=0.01 in Fig. 2). In contrast, the integration effect does not affect the establishment of the grating when $\tau_M \ll \tau_c$. In this case, the molecular-reorientational grating becomes τ independent if the laser fields are only characterized by phase fluctuation. For thermal sources with amplitude fluctuation, the coincidence of the intensity spikes between beams 1 and 2 gives rise to an enhancement of the amplitude of the molecular-reorientational grating at $\tau \approx 0$. More specifically, according to Eq. (9) we have $F_M(\tau) \propto 1 + \frac{2\alpha}{\gamma_M}\exp(-\gamma_M|\tau|)$ when $\gamma_M \gg \alpha$ (curve with $\gamma_M/\alpha = 100$ in Fig. 2).

In order to fully understand the RENFWM spectrum it is also necessary to consider the relative phase between $P_M(t)$ and $P_R(t)$. The situation is simple when beams 1 and 2 have narrow-band linewidth ($\gamma_M, \gamma_R \gg \alpha$). In this case, $A_1(t-t')A_2^*(t-t')$ and $A_2^*(t-t')$ in Eqs.(3) and (5) are slowly varying functions in comparison with $\exp(-\gamma_M t')$ and $\exp(-\gamma_R t')$, which have a peak at t'=0, and therefore can be approximated as $A_1(t)A_2^*(t)$ and $A_2^*(t)$, respectively. We have $P_M(t)$ and $P_R(t)$ proportional to $A_1(t)A_2^*(t)\int_0^\infty dt' A_3(t)\exp(-\gamma_M t')$ and $A_1(t)A_2^*(t)\int_0^\infty dt' A_3(t-t')\exp[-(\gamma_R - i\Delta)t')]$, respectively. Although the phases of $P_M(t)$ $P_R(t)$ and fluctuate randomly, the relative phase between them does

not depend on τ. The RENFWM spectrum should not change when τ is varied. More specifically, in the limit of $\gamma_M, \gamma_R \gg \alpha$, we have $I(\Delta,\tau) \propto \chi_M^2 + \chi_R^2 \frac{\gamma_R(\gamma_R+\alpha_3)}{(\gamma_R+\alpha_3)^2+\Delta^2} - 2\chi_M\chi_R \frac{\gamma_R\Delta}{(\gamma_R+\alpha_3)^2+\Delta^2}$.

Now, we consider the case where beams 1 and 2 have broadband linewidth ($\alpha \gg \gamma_M, \gamma_R \gg \alpha_3$). In the limit of $\alpha \gg \gamma_M, \gamma_R \gg \alpha_3$, we have

$$I(\Delta,\tau) \propto \chi_M^2 \exp(-2\alpha|\tau|) + \chi_R^2 \frac{\gamma_R\alpha}{\alpha^2+\Delta^2} - 2\chi_M\chi_R \left[\frac{2\gamma_M\gamma_R\alpha\Delta}{(\alpha^2+\Delta^2)^2} + \frac{\gamma_R\Delta}{\alpha^2+\Delta^2}\exp(-2\alpha|\tau|)\right].$$

At zero time delay no washout takes place in the establishment of the molecular-reorientational grating because $\Phi_M(\tau = 0)$ is stationary. On the other hand, due to the integration effect the fast random fluctuation of Φ_R, which is the Raman phase factor of $A_2^*(t-t')A_3(t-t')$ in Eq. (5), leads to the reduction of the amplitude of the Raman-active mode. As a result, compared with the case ($\gamma_M, \gamma_R \gg \alpha, \alpha_3$) the RENFWM spectrum exhibits a larger nonresonant background. We then increase τ so that beams 1 and 2 become uncorrelated. In this case, the randomization of $\Phi_M(\tau)$ washes out the molecular-reorientational grating. In contrast, $F_R(\Delta)$ is independent of τ.The implication of this is that the ratio between the nonresonant background and the Raman resonant signal decreases with inereasing τ when pump beams 1 and 2 have broadband linewidth. To make this clear we define a parameter $\eta(\tau) = F_R(\Delta)/F_M(\tau)$, which reflects the τ dependence of the ratio between the resonant and nonresonant signal intensities. For the narrow-band case ($\gamma_M, \gamma_R \gg \alpha, \alpha_3$), we have $\eta(\tau) \approx 1$. When the laser linewidths of beams 1 and 2 change from narrow band to broadband ($\alpha \gg \gamma_M, \gamma_R \gg \alpha_3$) η at zero time delay is reduced by a factor of about γ_R/α [i.e., $\eta(0) \approx \gamma_R/\alpha$]. Now we increase the time delay between beams 1 and 2. In the limit of $\tau \to \infty$, we have $\eta(\tau \to \infty) \to \infty$. Our numerical results are given in Figs. 3 and 4. Parameters used in Eq.(8) are $\chi_M/\chi_R = 0.35$, $\chi_T/\chi_R = 0.2$, $\gamma_R = 5 \times 10^{10}\text{sec}^{-1}$, $\gamma_M = 5\times10^{11}\text{sec}^{-1}$, $\gamma_T = 3\times10^{12}\text{sec}^{-1}$, $\alpha_3 = 2\times10^{10}\text{sec}^{-1}$; while $\alpha = 2 \times 10^{10}\text{sec}^{-1}$ for Fig. 3 and $1.8 \times 10^{11}\text{sec}^{-1}$ for Fig. 4. The time delays are $\tau = 0$ and 5600 ps ($\tau = 0$ and 1300 ps) for Figs. 3 (dashed curve) and 3 (solid curve) [Figs. 4 (dashed curve) and 4 (solid curve)], respectively. It is found from Fig. 3 that field correlation has little effect on the RENFWM spectrum when beams 1 and 2 have narrow bandwidth ($\alpha = 2 \times 10^{10}\text{sec}^{-1}$). The situations become quite different when beams 1 and 2 have broad bandwidth ($\alpha = 1.8 \times 10^{11}\text{sec}^{-1}$). Compared to the full correlation case [Fig. 4 (dashed curve)], the nonresonant background decreases and the intensity profile changes as beams 1 and 2 become uncorrelated [Fig. 4 (solid curve)].

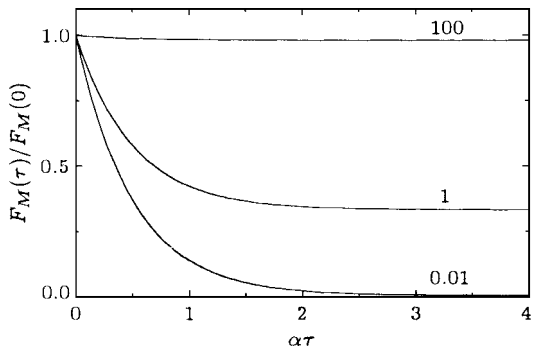


Fig.2. Theoretical curves of $F_M(\tau)/F_M(0)$ versus $\alpha\tau$. Here the values of γ_M/α, which equal 100, 1 and 0.01, are given.

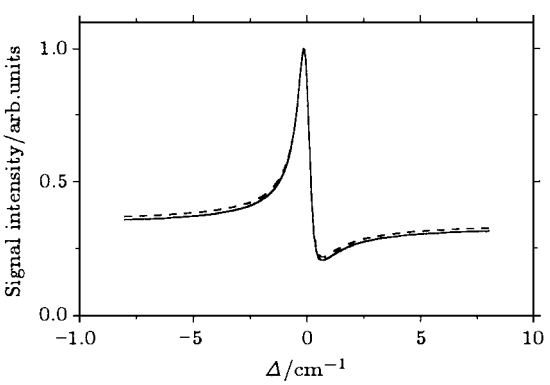


Fig.3. The RENFWM spectra at τ = 0ps (dashed curve) and 5600 ps (solid curve). Parameters: $\chi_M/\chi_R = 0.35$; $\chi_T/\chi_R = 0.20$; $\gamma_R = 5 \times 10^{10}\text{sec}^{-1}$; $\gamma_M = 5 \times 10^{11}\text{sec}^{-1}$; $\gamma_T = 3 \times 10^{12}\text{sec}^{-1}$, and $\alpha = \alpha_3 = 2 \times 10^{10}\text{sec}^{-1}$.

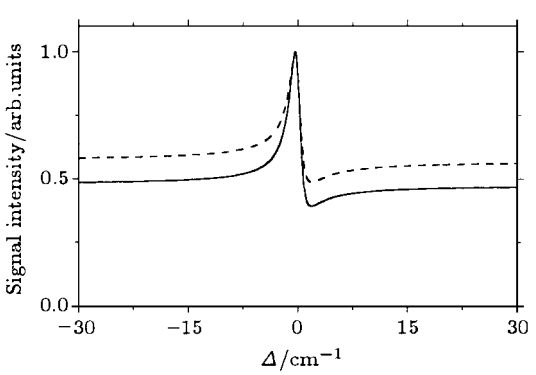


Fig.4. The RENFWM spectra at τ = 0ps (dashed curve) and 1300 ps (solid curve). Parameters: $\chi_M/\chi_R = 0.35$; $\chi_T/\chi_R = 0.20$; $\gamma_R = 5 \times 10^{10}\text{sec}^{-1}$; $\gamma_M = 5 \times 10^{11}\text{sec}^{-1}$; $\gamma_T = 3 \times 10^{12}\text{sec}^{-1}$; $\alpha = 1.8 \times 10^{11}\text{sec}^{-1}$ and $\alpha_3 = 2 \times 10^{10}\text{sec}^{-1}$.

For the sake of simplicity, we consider the Raman term again and neglect the contribution from

the molecular-reorientational grating and the thermal grating. By setting $\chi_M = \chi_T = 0$ in Eq. (8), we have $I(\Delta,\tau) \propto \chi_R^2 \frac{\gamma_R(\gamma_R+\alpha+\alpha_3)}{(\gamma_R+\alpha+\alpha_3)^2+\Delta^2}$, which originates from the phase fluctuation, is different from the result based on a chaotic model.[5,9] Our results are shown in Fig. 5 with $\gamma_R = 5\times10^{10}\mathrm{sec}^{-1}$, $\alpha_3 = 2\times10^{10}\mathrm{sec}^{-1}$, $\alpha = 1.8\times10^{11}\mathrm{sec}^{-1}$. The RENFWM spectrum has symmetrical line shape due to the elimination of the interference between the Raman resonant term and the nonresonant background originating solely from the molecular-reorientational grating.

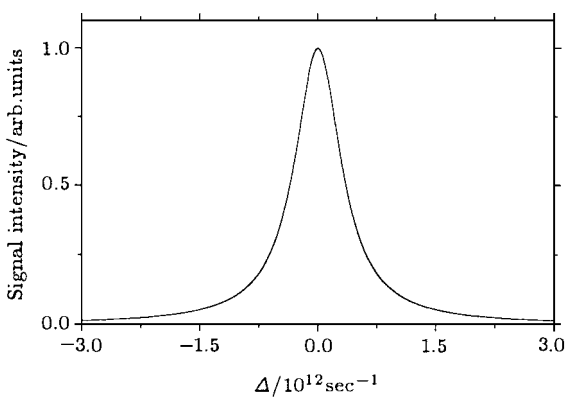


Fig.5. RENFWM spectrum at $\chi_M = \chi_T = 0$. Parameters: $\gamma_R = 5\times10^{10}\mathrm{sec}^{-1}$; $\alpha = 1.8\times10^{11}\mathrm{sec}^{-1}$ and $\alpha_3 = 2\times10^{10}\mathrm{sec}^{-1}$.

V. SECOND-ORDER COHERENCE FUNCTION THEORY OF RENFWM

Second-order coherence function theory is valid when we are only interested in the τ-dependent part of the RENFWM signal.[6] The FWM signal intensity can be well approximated by the absolute square of the stochastic average of the polarization $P_R(\boldsymbol{r},t)$, i.e., $I(\Delta=0,\tau) \propto |<P_R(\boldsymbol{r},t)>|^2$, which involves second-order coherence function in phase-conjugation geometry. Assuming that beams 1 and 2 have Gaussian line shape and beam 3 has much narrower linewidth so that it can be considered as a coherent light $[u_3(t)\approx 1, u_1(t)=u(t-\tau), u_2(t)=u(t)]$, then we have $<u(t_1)u^*(t_2)> = \exp\{-[\frac{\alpha}{2\sqrt{\ln2}}(t_1-t_2)]^2\}$, therefore

$$<P_R(\boldsymbol{r},t> = i\varepsilon_1(\varepsilon_2)^*\varepsilon_3 S(\boldsymbol{r},t)\chi_R\gamma_R\int_0^\infty \mathrm{d}t' \exp\left\{-\left[\frac{\alpha}{2\sqrt{\ln2}}(t'-\tau)\right]^2\right\}\exp(-\gamma_R t'). \quad (10)$$

The temporal behavior of the RENFWM can be understood from Eq. (10) directly. Figure 6 shows functions $\exp(-\gamma_R t')$ and $\exp\{-[\frac{\alpha}{2\sqrt{\ln2}}(t'-\tau)]^2\}$, where $\exp(-\gamma_R t')$ describes the decay of the Raman mode, while $\exp\{-[\frac{\alpha}{2\sqrt{\ln2}}(t'-\tau)]^2\}$ gives the mutual correlation between the Raman mode and the probe beam. Due to the integration effect, the nonlinear polarization is proportional to the integral over t' (from 0 to ∞) of the production of these two functions. Now, we discuss the relative time delay when the maximum of the RENFWM signal intensity occurs. The function $\exp\{-[\frac{\alpha}{2\sqrt{\ln2}}(t'-\tau)]^2\}$ can be divided into two parts: region I for $t'<\tau$ and region II for $t'>\tau$. When $\tau=0$, only region II has contribution to the integral. However, region I gives additional contribution to the integral when $\tau>0$. Therefore, the time delay at which RENFWM signal intensity is maximum $\tau_{\max}$ should not occur at 0, but shift to $\tau_{\max}>0$. When $\alpha \gg \gamma_R$ and $\tau>0$, we can approximate $\exp\left\{-\left[\frac{\alpha}{2\sqrt{\ln2}}(t'-\tau)\right]^2\right\}$ by a δ function,[10,11] i.e., $\exp\left\{-\left[\frac{\alpha}{2\sqrt{\ln2}}(t_1-t_2)\right]^2\right\} \approx \frac{2\sqrt{\pi\ln2}}{\alpha}\delta(t_1-t_2)$.

Then Eq.(10) becomes $<P_R(\boldsymbol{r},t)> = \varepsilon_1(\varepsilon_2)^*\varepsilon_3 S(\boldsymbol{r},t)\left[i\frac{2\chi_R\gamma_R\sqrt{\pi\ln2}}{\alpha}\exp(-\gamma_R|\tau|)\right]$, therefore

$$I(\Delta=0,\tau) \propto |<P_R(\boldsymbol{r},t)>|^2 = \frac{4\pi\ln2}{\alpha^2}|\varepsilon_1\varepsilon_2\varepsilon_3|^2\chi_R^2\gamma_R^2\exp(-2\gamma_R|\tau|). \quad (11)$$

Equation (11) indicates that the τ dependence of $I(\Delta=0,\tau)$ decays with a rate $2\gamma_R$. We then consider the case when $\tau<0$. In this case, the integral equation (10) involves only part of region II. Furthermore, the area of region II involved in the integral decreases with decay rate α as the time delay increases, therefore the τ dependence of the RENFWM signal reflects the coherence time of the laser. Figure 6 can also be used to discuss the case when $\alpha \ll \gamma_R$. In this limit, $\exp(-\gamma_R t')$ decays so rapidly that the integral in Eq. (10) is determined by the function $\exp\left\{-\left[\frac{\alpha}{2\sqrt{\ln2}}(t'-\tau)\right]^2\right\}$ at $t'=0$. In other words, $<P_R(\boldsymbol{r},t)>$ decays with rate α when $|\tau|$ increases. Physically, the relaxation time of the Raman mode is so short that the Raman mode excited by beam 2 and beam 3 should be probed immediately by beam 1. Hence, The temporal behavior of the RENFWM

reflects the mutual correlation between beams 1 and 2. Finally, we note that according to the above discussion, no coherence spike exists at τ=0, which is different drastically from the corresponding CSRS with incoherent light.[12]

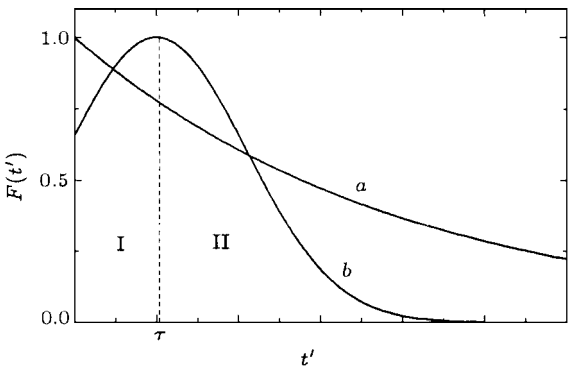


Fig.6. Schematic to describe the second-order coherence function theory of RENFWM. $F(t') = \exp(-\gamma_R t')$ for curve (a) and $F(t') = \exp\left\{-[\frac{\alpha}{2\sqrt{\ln 2}}(t'-\tau)]^2\right\}$ for curve (b).

VI.DISCUSSION AND CONCLUSION

In this paper, we assumed that the laser sources are phase-diffusing models, which are used to describe an amplitude-stabilized laser source with Lorentzian line shape. This model assumes that the amplitude of the laser field is a constant, while its phase fluctuates as random process. We have employed phase-diffusion model to study the effects of laser field correlation on RENFWM. The different roles of the field fluctuations have been pointed out. A time-delayed method has been proposed to suppress the thermal background. An enhancement of the ratio between the resonant and nonresonant RENFWM signal intensities is found as the time delay is increased when the laser has broadband linewidth. This enhancement can be explained by considering that the field fluctuations have different effects on the Raman resonance and on the laser-induced molecular-reorientational grating. When the lasers have Gaussian line shape, we also present a second-order coherence function theory to elucidate the temporal asymmetry behavior of the RENFWM.

REFERENCES

[1] Y. P. Zhang, T. T Tang, L. Q. Sun and P. M. Fu, *Phys. Rev.*, **A61**(2000),3809.
[2] N. Morita and T. Yajima, *Phys.Rev.*, **A30**(1984),2525.
[3] S. Asaka, M. Nakatsuka, M. Fujiwara and M. Matsuoke, *Phys. Rev.*, **A29**(1984),2286.
[4] M. H. Anderson, G. Vemuri, J. Cooper, P. Zoller and S. J. Smith, *Phys. Rev.*, **A47**(1993),3202.
[5] P. M. Fu, Z. H. Yu, X. Mi, Q. Jiang and Z. G. Zhang, *Phys. Rev.*, **A46**(1992),1530.
[6] X. Mi, Z. Yu, Q. Jiang and P. Fu, *Phys. Rev.*, **A48**(1993), 3203.
[7] D. DeBeer, V. G. Van Wagenen, R. Beach and S. R. Harmann, *Phys. Rev. Lett.*, **56**(1986),1128.
[8] B. Picinbono and E. Boileau, *J. Opt. Soc. Am.*, **58**(1968), 784.
[9] Y. P. Zhang, L. Q. Sun, T. T Tang, L. Zhang and P. M. Fu, *Chin. Phys. Lett.*, **17**(2000),206.
[10] Y. P. Zhang, T. T Tang and P. M. Fu, *Acta Physica Sinica* **48**(1999),242(in Chinese).
[11] Y. P. Zhang, C. L. Gan, J. P. Zhu, T. T Tang and P. M. Fu, *Acta Physica Sinica* **48**(1999),1667(in Chinese).
[12] T. Hattori, A. Terasaki and T. Kobayashi, *Phys. Rev.*, **A35** (1987),715.